

Research

Critical assessment of the lattice Boltzmann method for cavitation modelling based on single bubble dynamics

Xin Xiong¹ · Tom-Robin Teschner¹ · Irene Moulitsas¹ · Tamás István Józsa¹

Received: 11 March 2024 / Accepted: 15 April 2024

Published online: 01 May 2024

© The Author(s) 2024 [OPEN](#)

Abstract

The lattice Boltzmann Method (LBM) is recognised as a popular technique for simulating cavitation bubble dynamics due to its simplicity. In the validation of LBM results, the Rayleigh-Plesset (R-P) equation is commonly employed. However, most studies to date have neglected the impact of simulation settings on the predictions. This article sets out to quantify the impact of LBM domain size and bubble size, and the initial conditions of the R-P equations on the predicted bubble dynamics. First, LBM results were validated against the classical benchmarks of Laplace's law and Maxwell's area construction. LBM results corresponding to these fundamental test cases were found to be in satisfactory agreement with theory and previous simulations. Secondly, a one-to-one comparison was considered between the predictions of the LBM and the R-P equation. The parameters of the two models were matched based on careful considerations. Findings revealed that a good overlap between the predictions is observable only under certain conditions. The warming-up period of the LBM simulations, small domain size, and small bubble radius were identified as key factors responsible for the measured differences. The authors hope that the results will promote good simulation practices for cavitation simulation including both single bubbles and bubble clusters.

Article Highlights

- Integrating different initial conditions from the lattice Boltzmann Method (LBM) into the Rayleigh-Plesset (R-P) equation shows notable difference results.
- The size of the domain and the distance between the centre of the circular bubble and its boundary are crucial factors in ensuring alignment between the results obtained from the LBM and the R-P equation.
- There is an approximately linear relationship between the radius of the bubble and the iteration at which the difference between the LBM and the R-P equation reaches a 5% threshold.

Keywords Lattice Boltzmann simulation · Rayleigh-Plesset equation · Single bubble

1 Introduction

Cavitation is a phenomenon that involves the transition from liquid to vapour due to a decrease in pressure, leading to the formation of vapour bubbles within the liquid. This phenomenon occurs in many hydrodynamic machines, where the collapse of cavitation bubbles can generate high pressure and high temperature, resulting in noise,

✉ Xin Xiong, xin.xiong@cranfield.ac.uk | ¹Centre for Computational Engineering Sciences, Cranfield University, Cranfield MK43 0AL, UK.



Discover Applied Sciences

(2024) 6:241

| <https://doi.org/10.1007/s42452-024-05895-1>

vibration, and erosion. However, cavitation can be leveraged to enhance heat transfer and for applications such as drilling petroleum wells, where micro-jets induced by the collapse of bubbles play a crucial role [1].

Numerous numerical attempts have been made to simulate cavitation bubbles using traditional macroscopic methods based on the Navier-Stokes equation [2–4]. In addition, due to its advantages in simulating multiphase models, Lattice Boltzmann Method (LBM) has also been applied to bubble simulation [5–7]. Within the LBM framework, at least four different approaches are known: (i) colour-gradient model; (ii) free energy model; (iii) phase-field model; and (iv) Shan-Chen model. Colour gradient model is popular when it comes to immiscible flow [8–11]. Free energy model and phase field model usually comes with Cahn-Hilliard equation [12] and Allen-Cahn equation [13] for tracking the interface and they are popular in cases such as Rayleigh-Taylor instability [14–16].

Among these approaches, the Shan-Chen model has gained popularity due to its simplicity and effectiveness in simulating bubble dynamics. This model employs a potential to mimic the interaction between particles, adding force to the velocity to trigger phase separation [17]. For instance, numerous articles focus on studying a single bubble near a solid wall based on the Shan-Chen model [18–20]. Furthermore, simulations of a bubble near a concave wall and a bubble near a solid particle [5] have also been conducted. The advantages of the Shan-Chen model include its ability to easily incorporate the equation of state and facilitate the automatic separation of phases and components.

In articles studying bubble dynamics based on the Shan-Chen model, the validation of bubble growth or collapse was conducted by comparing the Rayleigh-Plesset (R-P) equation with LBM simulation results. Shi et al. [21] compared the R-P equation with LBM simulation results for a bubble radius of 20 lattice units, focusing on growth and collapse. The simulation domain size was 2000x2000x1000, but the article did not provide a detailed analysis of the influence of the boundary effect. Ezzatneshan and Vaseghnia [22] also validated LBM results for the same radius against the R-P equation under different pressures, determining the critical pressure for bubble growth or collapse. However, their study considered solely a radius of 15 lattice units, and the influence of different radii was not explored. Visual observation of the reported results suggests discrepancies between predictions of the LBM and R-P equation, especially in the case of collapsing bubbles near the end of the simulation time when the bubble radii become comparable to the lattice size. However, it remains unclear when such effects start to become significant.

Peng et al. [1] compared LBM results with variable boundary pressure against the relevant R-P equation, demonstrating good agreement with slight deviations at the beginning. This suggests that initial conditions significantly influence the results. In another study, Peng et al. [23] investigated LBM results with different pressure differences and radii against the R-P equation. While results were satisfactory in certain iterations, small deviations were observed.

Based on the aforementioned studies, it is clear that there is a lack of quantitative understanding regarding the impact of simulation parameters on the predicted bubble dynamics trends. It is also crucial to recognize that the LBM and the R-P equation provide solutions to the same physical problem in different mathematical frameworks. The two methods have a different set of input parameters and a different set of output variables which make fair comparison challenging. To the authors' knowledge, a detailed description has not been provided to date on how to address this challenge and how it impacts the outcome of the comparison. Specifically, there is a lack of comprehensive analyses regarding the influence of different bubble radii, and detailed investigations into the effects of initial conditions and domain size on LBM simulations in the context of bubble dynamics based on the Shan-Chen model. In addition, previous studies are challenging to reproduce because of the lack of publicly available repositories of the LBM with cavitation modelling.

The primary aim of this article is to undertake a critical assessment of the lattice Boltzmann method concerning its application to single bubble dynamics and, in turn, to establish a foundational framework for the simulation of bubble clusters. To realize this aim, the article is structured as follows. In section two, the mathematical frameworks underpinning the simulations are outlined, encompassing relevant equations and providing details of the problem statement and configuration. This section also describes the three investigated test cases: Laplace's law validation, Maxwell's area construction validation, and R-P equation validation. Section three presents the results of the validation cases alongside a discussion regarding the impact of various parameters. Finally, conclusions are summarised in section four. Additionally, this study addresses a notable gap by publicly releasing a 2D repository

2 Methods

2.1 Description of the lattice Boltzmann method

In this article, a two-dimensional $D2Q9$ model was implemented based on the Shan-Chen multiphase model. The additional force was considered through the velocity shifting method by modifying the equilibrium velocity, without any alteration to the lattice Boltzmann equation, expressed in [24] as

$$f_i(\mathbf{x} + \mathbf{e}_i \Delta t, t + \Delta t) - f_i(\mathbf{x}, t) = -\frac{1}{\tau} [f_i(\mathbf{x}, t) - f_i^{eq}(\mathbf{x}, t)]. \quad (1)$$

Here, i represents one of the nine directions, f is the probability density function, \mathbf{x} and t are the coordinates in space and time, Δt is the time step, \mathbf{e}_i is the unit vector direction of the lattice, τ is the relaxation time and f^{eq} is the equilibrium probability distribution function. The relation of relaxation frequency, lattice viscosity, and relaxation time is $\omega = 3\nu^{LB} + 0.5 = 1/\tau$ [25]. Numerical tests showed that a relaxation frequency of $\omega = 1$ provided acceptable stability and is chosen throughout this study. This setting is also found in the literature [1, 21, 23], further proving its justification. The "LB" and "RP" superscripts are used to distinguish quantities that appear in both the Lattice Boltzmann (LB) and Rayleigh-Plesset (RP) equations.

The equilibrium probability distribution function can be expressed as [25]

$$f_i^{eq}(\mathbf{x}, t) = w_i \rho(\mathbf{x}) \left[1 + \frac{3\mathbf{e}_i \cdot \mathbf{u}}{c^2} + \frac{9(\mathbf{e}_i \cdot \mathbf{u})^2}{2c^4} - \frac{3\mathbf{u}^2}{2c^2} \right], \quad (2)$$

where the weights w_i are equal to 4/9 for $i = 0$, 1/9 for $i = 1$ to 4, and 1/36 for $i = 5$ to 9. The lattice speed is denoted by c , whereas ρ and \mathbf{u} are the macroscopic density and the velocity vector. The unit vectors \mathbf{e}_i correspond to the nine propagation directions.

According to Shan and Chen [26], the additional force required to describe multiphase flows can be expressed as

$$\mathbf{F}(\mathbf{x}, t) = -G\psi(\mathbf{x}, t) \sum_{i=0}^8 \omega_i \psi(\mathbf{x} + \mathbf{e}_i t, t) \mathbf{e}_i, \quad (3)$$

where G denotes the interaction strength between particles, it is eliminated during the computations and therefore G does not affect the results [21]. And ψ represents the effective density. Additionally, the velocity shifting method was implemented to enhance stability [24] so that

$$\mathbf{u}^{eq} = \frac{1}{\rho} \left(\sum_i f_i \mathbf{c}_i + \tau \mathbf{F} \right), \quad (4)$$

where \mathbf{F} represents the Shan-Chen force vector and \mathbf{u}^{eq} is the equilibrium velocity vector. Furthermore, the Carnahan-Starling (C-S) Equation of State (EOS) is incorporated by modifying the effective density [21] according to

$$\psi = \sqrt{\frac{2}{Gc_s^2} (p - \rho c_s^2)}. \quad (5)$$

Here, c_s denotes the speed of sound and p is the static pressure [1] governed by the C-S EOS:

$$p = \rho R_c T \frac{1 + b\rho/4 + (b\rho/4)^2 - (b\rho/4)^3}{(1 - b\rho/4)^3} - a\rho^2. \quad (6)$$

The corresponding coefficients and the universal gas constant are chosen as $a = 1$, $b = 4$, and $R_c = 1$. The carried-out simulations rely on the assumption of isothermal flow condition. Unless stated otherwise, the critical temperature is $T_c = 0.09433$, and the ratio of the temperature and the critical temperature is set to $T/T_c = 0.75$. The same settings determined based on the critical pressure, density, and temperature were employed in several former studies [5, 21].

There are certain literature [5, 21, 23] that use the original Shan–Chen model, which is similar to the model in this article, and compare it with the R-P equation. An excellent agreement was found in all of their test cases. In addition, alternative models exist. For example, the Multi-Relaxation-Time model (MRT) was performed by Gai et al. [27] and by Ezzatneshan and Vaseghnia [28]. Furthermore, Peng et al. [1] proposed a two-layer lattice scheme for the interaction force. The advantage of the MRT model lies in its increased stability. In addition, the multi-range force model has a better gas-liquid density ratio [29]. However, these advantages appear to have little impact on the test cases considered in this study based on the existing literature [21, 28]. Considering bubble growth and collapse, excellent agreement was reported both with the original [5, 21, 23] and the enhanced [1] Shan–Chen models.

This study focuses solely on the two-dimensional LBM simulation so that the computational domain is rectangular in every case. The implementation was built upon a publicly available code detailed in [24].

2.2 Description of Rayleigh-Plesset equation

The R-P equation is provided in a cylindrical coordinate system to match the two-dimensional LBM configuration. Considering the incompressible continuity and momentum equations as discussed in [30], the R-P equation takes the form of

$$\ddot{R}^{\text{RP}} = \frac{1}{\ln(R_\infty/R^{\text{RP}}) \cdot R^{\text{RP}}} \left[\frac{p_g^{\text{RP}} - p_\infty}{\rho_l^{\text{RP}}} - \frac{\sigma^{\text{RP}}}{\rho_l^{\text{RP}} R^{\text{RP}}} - \frac{2\nu^{\text{RP}}}{R^{\text{RP}}} \dot{R}^{\text{RP}} + \frac{1 - (R^{\text{RP}}/R_\infty)^2 - 2 \ln(R_\infty/R^{\text{RP}})}{2} (\dot{R}^{\text{RP}})^2 \right]. \quad (7)$$

Here, R^{RP} is the bubble radius as a function of time which is the primary variable. \dot{R}^{RP} and \ddot{R}^{RP} are the first and second temporal derivatives of the radius, respectively. R_∞ is the distance between the centre of the circular bubble and a circular boundary where constant p_∞ pressure is assumed. The surface tension, kinematic viscosity, and liquid density are denoted by σ^{RP} , ν^{RP} , and ρ_l^{RP} , respectively. p_g^{RP} is the gas (vapour) pressure.

Numerical solutions of the Rayleigh-Plesset equation were obtained with MATLAB [31]. To this end, the Dormand-Prince method [32] was used as implemented in the “ode45” function which requires $R^{\text{RP}}(t = 0)$ and $\dot{R}^{\text{RP}}(t = 0)$ as initial conditions.

2.3 Comparison of the mathematical framework of the lattice Boltzmann and the Rayleigh-Plesset equations

Chapman-Enskog procedure [33] provides a bridge between the Boltzmann and Navier–Stokes equations by proving that the continuum formulation follows from the lattice Boltzmann equations. However, in the transition from non-dimensional to dimensional systems, mismatches often arise. This issue can be resolved based on similarity conditions [24]. In terms of cavitation flows, non-dimensional groups have been identified using Buckingham’s π theorem [34].

For example, $\pi = \frac{\sqrt{p_\infty} R}{\nu}$ can be one of the dimensionless groups. However, in the literature [5, 23, 27, 28] investigating cavitation based on LBM, an alternative solution is used extensively where lattice units are substituted into the RP equation. For this reason, the same procedure was followed in this article. For future research, it would be beneficial to study physically realisable cases based on similarity conditions.

The lattice Boltzmann equation imposes a combined Initial Value Problem (IVP) and Boundary Value Problem (BVP) to cover flow physics in the domain of interest Ω investigated in a rectangular coordinate system as shown in Fig. 1. From a macroscopic point of view, the initial conditions describe the density and velocity vector fields at the beginning of the observation. In the case of cavitation simulations, initial conditions are set based on the initial bubble radius, and liquid and gas (vapour) density. Boundary conditions require the prescription of the density and velocity vectors at every considered time instant at the domain boundary denoted by $\partial\Omega$.

In the case of the LBM, the bubble radius R^{LB} can be estimated by assuming that the bubble surface is located where the density is equal to the average density of the liquid and gas phases $(\rho_l^{\text{LB}} + \rho_g^{\text{LB}})/2$. In the case of the LBM, liquid density ρ_l^{LB} is computed by averaging the macroscopic density at a significant distance from the bubble. The gas density ρ_g^{LB} is

Table 1 Comparison between the mathematical frameworks employed in the lattice Boltzmann method and the Rayleigh-Plesset equation

	LBM	R-P equation
Physical approach	Non-dimensional Boltzmann equation (statistical mechanics)	Dimensional Navier-Stokes equation (continuum mechanics)
Type of governing equations	Initial and boundary value problem	Initial value problem
Variables	$\rho(\mathbf{x}, t), \mathbf{u}(\mathbf{x}, t)$	$R(t)$
Two-dimensional coordinate system	Cartesian	Cylindrical
Bubble interface	Smooth and estimated	Exact and sharp
Boundary distance	Average radial distance of bounding rectangle	Exact radial distance
Initial condition	$\rho(\mathbf{x}, t = 0), \mathbf{u}(\mathbf{x}, t = 0)$	$R(t = 0), \dot{R}(t = 0)$
Boundary condition	$\rho(\mathbf{x} \in \partial\Omega, t), \mathbf{u}(\mathbf{x} \in \partial\Omega, t)$	N/A
Parameters	$\nu, L_x, L_y, a, b, c, R_c, T, T_c$	$\nu, R_\infty, \sigma, \rho_l, \rho_g, p_\infty$
Radius	Calculated based on macroscopic density	Direct numerical result from equation

calculated as an average of the density values at the four central lattices inside the bubble. The liquid and gas pressures are determined following the same strategy.

By comparison, the Rayleigh-Plesset equation is an IVP describing bubble dynamics in a cylindrical coordinate system in this study. To ensure comparability between the solutions obtained from the LBM and the R-P equation, the parameters defining the two problems need to be matched as closely as possible. It is worth noting that because of the mismatching mathematical framework between the lattice Boltzmann and Rayleigh-Plesset equations, there can be multiple ways to match model parameters. Furthermore, it is important to highlight that the details of these calculations were consistently missing from previous publications [5, 23, 27, 28].

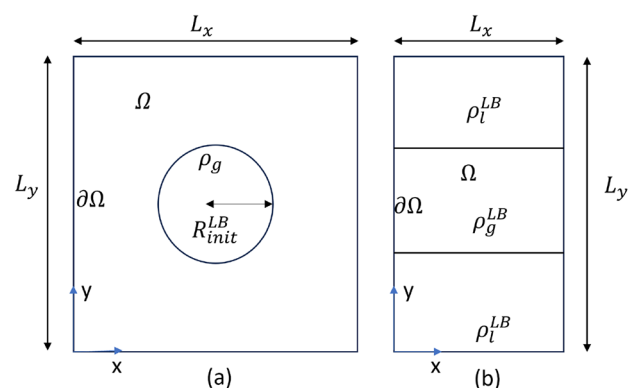
The parameters required to solve the R-P equation are obtained from the settings and results of LBM simulations as detailed below. Considering that the kinematic viscosity appears in both Eq. (7) and Eq. (1) (indirectly through the relaxation time), this parameter can be matched directly by setting $\nu^{\text{RP}} = \nu^{\text{LB}}$. Furthermore, the liquid and gas densities and pressures can be matched once they are determined from the LBM simulation as described above: $\rho_l^{\text{RP}} = \rho_l^{\text{LB}}, \rho_g^{\text{RP}} = \rho_g^{\text{LB}}, p_g^{\text{RP}} = p_g^{\text{LB}}, p_\infty = p_l^{\text{LB}}$. Imposing initial conditions for the R-P equation is also relatively straightforward:

$$\begin{aligned} R^{\text{RP}}(t = 0) &= R^{\text{LB}}(t_{\text{ex}}), \\ \dot{R}^{\text{RP}}(t = 0) &= \dot{R}^{\text{LB}}(t_{\text{ex}}), \end{aligned} \quad (8)$$

Here, t_{ex} is the time instant corresponding to information exchange from the LBM simulation to the R-P equation. The temporal derivative of the radius from the LBM (\dot{R}^{LB}) is calculated based on the first-order forward Euler scheme.

Calculating R_∞ is non-trivial because of the mismatching coordinate systems. Considering the square-shaped LBM domain shown in Fig. 1a, R_∞ can be estimated as the average distance between the boundary and the bubble centre:

Fig. 1 Problem statement of the simulation **a** bubble simulation **b** flat interface simulation



$$R_{\infty} = \frac{1}{\pi/4} \int_0^{\pi/4} \left(\frac{0.5 \cdot L_x}{\cos \alpha} \right) d\alpha = \frac{2L_x}{\pi} \log(\sqrt{2} + 1). \quad (9)$$

Finally, determining σ_{RP} is also non-trivial because the surface tension can be obtained from the LBM only after post-processing. According to Laplace's law [22, 35, 36], surface tension can be expressed as

$$\sigma^{LB} = R^{LB} \cdot (\rho_l^{LB} - \rho_g^{LB}). \quad (10)$$

Here, R^{LB} , ρ_l^{LB} , and ρ_g^{LB} correspond to a steady state solution of the LBM where the bubble reached equilibrium. Thereafter, $\sigma^{RP} = \sigma^{LB}$ is set.

Table 1 lists the key differences between the LBM and the R-P equation. To compare the results obtained by these two methods, the relative radius difference is introduced as

$$\Delta R = \frac{R^{LB} - R^{RP}}{R^{RP}}. \quad (11)$$

In the following sections, the results will be analysed to shed light on the key factors which cause differences between LBM and R-P equation predictions in terms of bubble dynamics. After matching the parameters of the two models, the first time point corresponding to $\Delta R > 5\%$ is identified to assess the interval within which predictions overlap relatively well.

2.4 Problem statement and the test cases

LBM simulations take place in a two-dimensional rectangular domain denoted by Ω bounded by the $\partial\Omega$ curve as mentioned earlier. The domain size is determined by the x-directional and y-directional sizes L_x and L_y . In the following, case descriptions are provided summarising the initial and boundary conditions for the macroscopic velocity \mathbf{u} and density ρ . This study uses periodic boundary conditions or boundary conditions with prescribed velocity and density based on the full-way bounce-back condition. The latter is established with a full-way bounce-back boundary condition [25] imposed on the probability density functions f . The EOS governed by Eq. (6) provides a unique relationship between density ρ and the pressure p , so that boundary conditions can be also formulated for p instead of ρ .

2.4.1 Flat interface case

In the flat interface case, the width of the domain Ω , L_x , is set to 20 (lattice length unit) l.u., and the height, L_y , to 200 l.u. In the middle of the domain, a layer with gas phase is initialised with macroscopic density ρ_g^{LB} . At the top and the bottom, the liquid phase is present, where initial density ρ_l^{LB} is implemented. In the flat interface simulations, periodic boundary conditions are enforced along the x and y directions at $\partial\Omega$. In addition, the interface between the liquid and gas phases is smoothed following the configuration of Huang et al. [37] as

$$\rho(y) = \rho_g^{LB} + \frac{\rho_l^{LB} - \rho_g^{LB}}{2} \times \text{abs} \left\{ \begin{aligned} & \tanh \left[\frac{2(y - 50)}{5} \right] \\ & - \tanh \left[\frac{2(y - 150)}{5} \right] \end{aligned} \right\}, \quad (12)$$

During this test case, the critical temperature is kept constant while the temperature is changed. After reaching the equilibrium state, the densities of liquid and gas were recorded for every temperature. The equilibrium state is defined as the condition when the change in density between two iterations is less than 10^{-4} [m.u. · l.u.⁻³]. To be more clear, the initial condition and boundary condition of this case is summarized as follows,

- there are 2 liquid layers with a vapour layer between them as shown in Fig. 1.
- The initial density is given by Eq. (12)
- the initial velocity vector is $\mathbf{0}$

- periodic boundary conditions are imposed in both the x and the y directions

2.4.2 Bubble equilibrium case

In the bubble equilibrium case, L_x and L_y are equal, forming a square domain in region Ω . Inside the bubble, the gas pressure p_g^{LB} and the density of gas ρ_g^{LB} are set. Different bubble radii R^{LB} are set. In this case, a periodic boundary condition is enforced in both x and y direction and three radii of 20 [l.u.], 25 [l.u.], 30 [l.u.] with a domain size of 100 [l.u.] is set. An initial smooth interface with initial radius R_{init}^{LB} was implemented on the bubble interface with 5 lattices for better stability according to Peng et al. [1].

$$\rho(x, y) = \frac{\rho_l^{LB} + \rho_g^{LB}}{2} + \frac{\rho_l^{LB} - \rho_g^{LB}}{2} \cdot \tanh \left(\frac{2(\sqrt{(x - 0.5 \cdot L_x)^2 + (y - 0.5 \cdot L_y)^2} - R_{init}^{LB})}{5} \right) \quad (13)$$

The initial and boundary conditions of Laplace's law validation case are as follows,

- The initial density is given by Eq. (13)
- the initial velocity vector is $\mathbf{0}$
- periodic boundary conditions are imposed in both the x and the y directions

2.4.3 Bubble growth and collapse

In this case, a full-way bounce-back boundary condition with a constant pressure boundary condition was implemented to validate the R-P equation. A smooth interface was also implemented based on Eq. (13). The equilibrium densities of the liquid and gas, taken from Maxwell's area construction based on the C-S EOS, are 0.33 and 0.011, respectively. To trigger the growth and collapse of the bubble, densities different from the equilibrium density of the liquid on the boundary were implemented, which are 0.34 for collapse and 0.31 for growth, respectively. Furthermore, 1000 time steps were simulated for a sufficiently long time for bubble growth and collapse. The domain size for the bubble simulation is set to be square, including 100 [l.u.], 200 [l.u.], 400 [l.u.] and 1000 [l.u.]. The initial $\mathbf{u} = \mathbf{0}$ and boundary condition of bubble case with prescribed density boundary condition (ρ , also prescribed pressure p as dictated by the EOS presented in Eq.(6)) are as follows,

- The initial density is given by Eq. (13)
- the initial velocity vector is $\mathbf{0}$
- full-way bounce-back boundary conditions are imposed in both the x and the y directions

Table 2 Parameters of the test cases conducted with the lattice Boltzmann method to investigate single bubble dynamics

	Domain Size ($L_x = L_y$ [l.u.])	Radius [l.u.]	Density [m.u. · l.u. ⁻³]
case1-4	100, 200, 400, 1000	20	0.31
case5-8	100, 200, 400, 1000	20	0.34
case9-13	100, 200, 400, 1000	25	0.31
case14-17	100, 200, 400, 1000	25	0.34
case18-21	100, 200, 400, 1000	30	0.31
case22-25	100, 200, 400, 1000	30	0.34
case26-29	100, 200, 400, 1000	35	0.31
case30-32	100, 200, 400, 1000	35	0.34
case33	1000	350	0.34

To analyse the impact of domain size, radius, and boundary condition in the bubble case with constant pressure boundary condition, different cases were tested as listed in Table 2.

3 Results and discussion

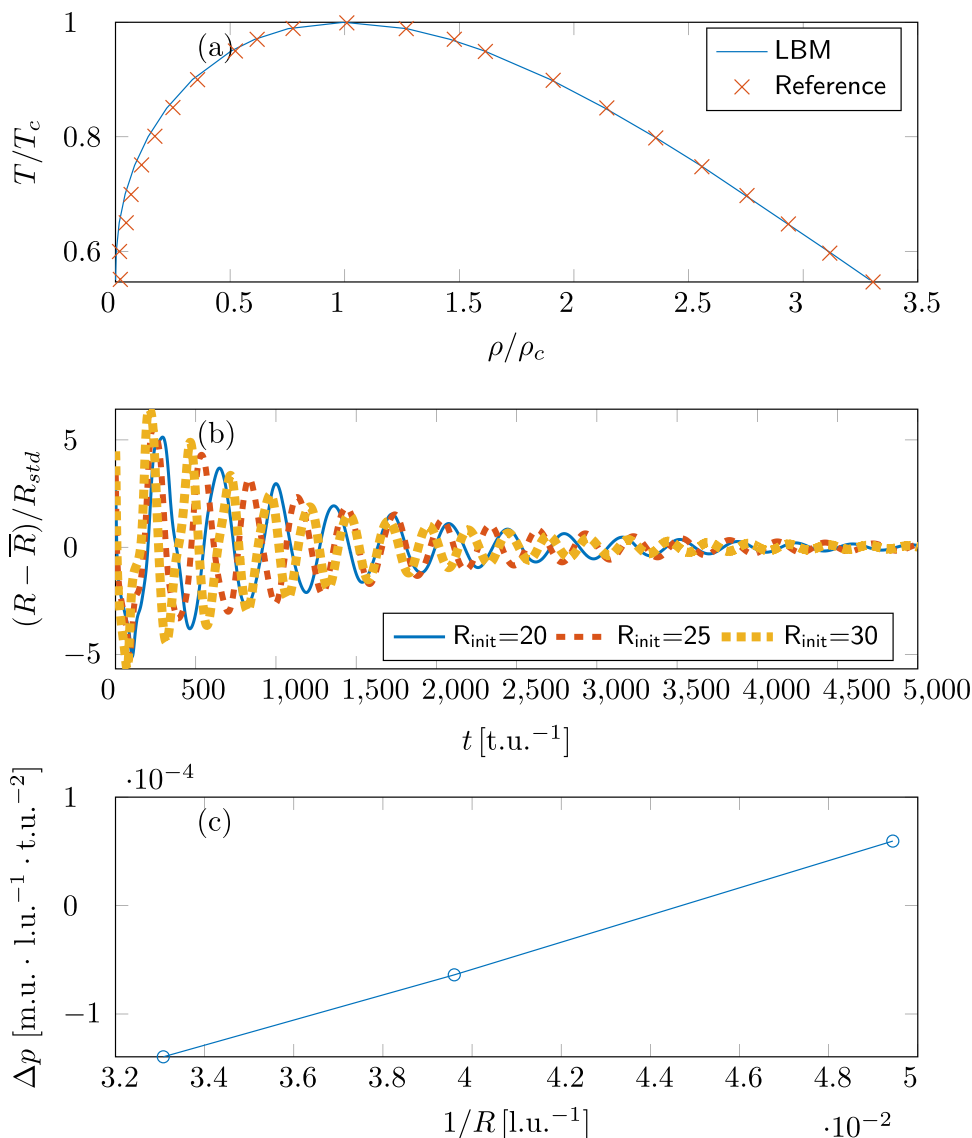
3.1 Maxwell’s area construction validation

To validate the thermodynamic consistency, the Maxwell’s Area construction was validated. For simplicity, the reference data were digitised from Peng et al. [1]. As can be seen from Fig. 2a, the LBM results are close to the reference data, which validates our code for thermodynamic consistency.

3.2 Laplace’s law validation

As can be seen from Fig. 2b, the bubble gradually evolves to the equilibrium state with periodic boundary conditions. As can be seen from Fig. 2c, the results from LBM are in satisfactory agreement with the Laplace’s law. The results also

Fig. 2 Laplace’s law and Maxwell’s Area Construction, reference data from Peng et al. [1] **a** Maxwell’s area Construction **b** different bubble radius simulation **c** Laplace’s law validation

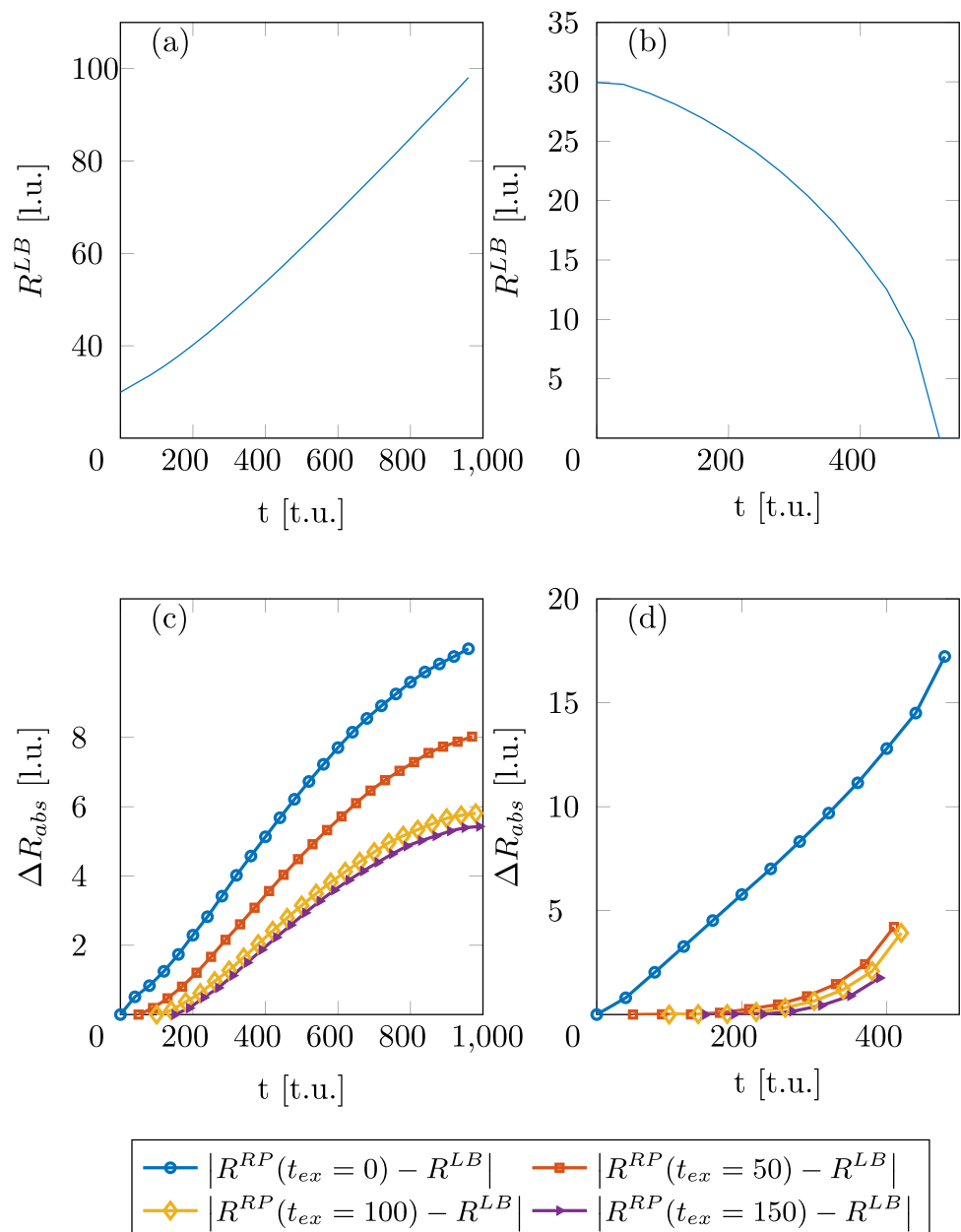


agree well with previous findings [27, 28]. As suggested by Equation (10), the slope of the line presented in Fig. 2c is used to obtain the surface tension from the LBM simulation. This parameter was then provided as input to simulations based on the R-P equation detailed in the next section.

3.3 The impact of initial condition

Figure 3 a and b state that the trends agree qualitatively well with previous observations regarding bubble growth and collapse in the case of the LBM [23, 28]. The outcomes obtained under distinct initial conditions of the R-P equation in Fig. 3c and d manifest a noteworthy influence on the validation of LBM against the R-P equation. Particularly in the case of collapse scenarios, the R-P equation with the initial condition of LBM at time zero exhibits deviation in the initial stages. The observed trend indicates that with an increase in the iterations from the initial condition in LBM, the difference between LBM and R-P diminishes. This phenomenon may be attributed to the need for fluid flow to develop inside the domain to ‘wash out’ the effect of the initial condition and thus reach a physically relevant state. It is worth recognising that the difference between R-P and LBM predictions is increasing monotonically as a

Fig. 3 The impact of initial condition. R-P equation with initial condition of LBM at time 0, 50, 100, 150 [t.u.]. Where R^{LB} is the radius of LBM results and $R^{RP}(t_{ex} = 0)$, $R^{RP}(t_{ex} = 50)$, $R^{RP}(t_{ex} = 100)$, $R^{RP}(t_{ex} = 150)$ are the initial radius of R-P equation with time instant (0, 50, 100, 150) [t.u.] which corresponding to information exchange from the LBM simulation to the R-P equation. $|R^{RP}(t_{ex}) - R^{LB}|$ denotes the absolute radius difference (ΔR_{abs}) between LBM and R-P equation. **a** growth case **b** collapse case **c** absolute radius difference of growth case **d** absolute radius difference of collapse case



function of time in every case. Notably, in the investigation conducted by Peng et al. [1], disparities are noted at the initial stages despite the implementation of variable pressure boundary conditions.

However, initializing the R-P equation with LBM conditions at $t_{ex} = 100$ [t.u.] and $t_{ex} = 150$ [t.u.] yields a considerably smaller difference. The marginal reduction in difference when moving from an initial condition at $t_{ex} = 100$ [t.u.] to $t_{ex} = 150$ [t.u.] suggests that $t_{ex} = 100$ [t.u.] is a sufficiently late time point for initializing the R-P equation for subsequent comparisons. This decision is supported by the minimal additional accuracy gain observed at $t_{ex} = 150$ [t.u.], indicating that $t_{ex} = 100$ [t.u.] serves as an appropriate and pragmatic choice for initial conditions in later comparative analyses. In the study conducted by Ezzatneshan and Vaseghnia [28], the graphical comparison between the LBM and the R-P equation, particularly in the context of minimal pressure differences, reveals a significant difference between the two methods during the initial stages, underscores a notable difference at the initial stages. This discrepancy clearly shows how initial conditions significantly impact the validation and accuracy of the LBM compared to the R-P equation, underlining their crucial role in computational modelling and method comparison.

3.4 The impact of domain size

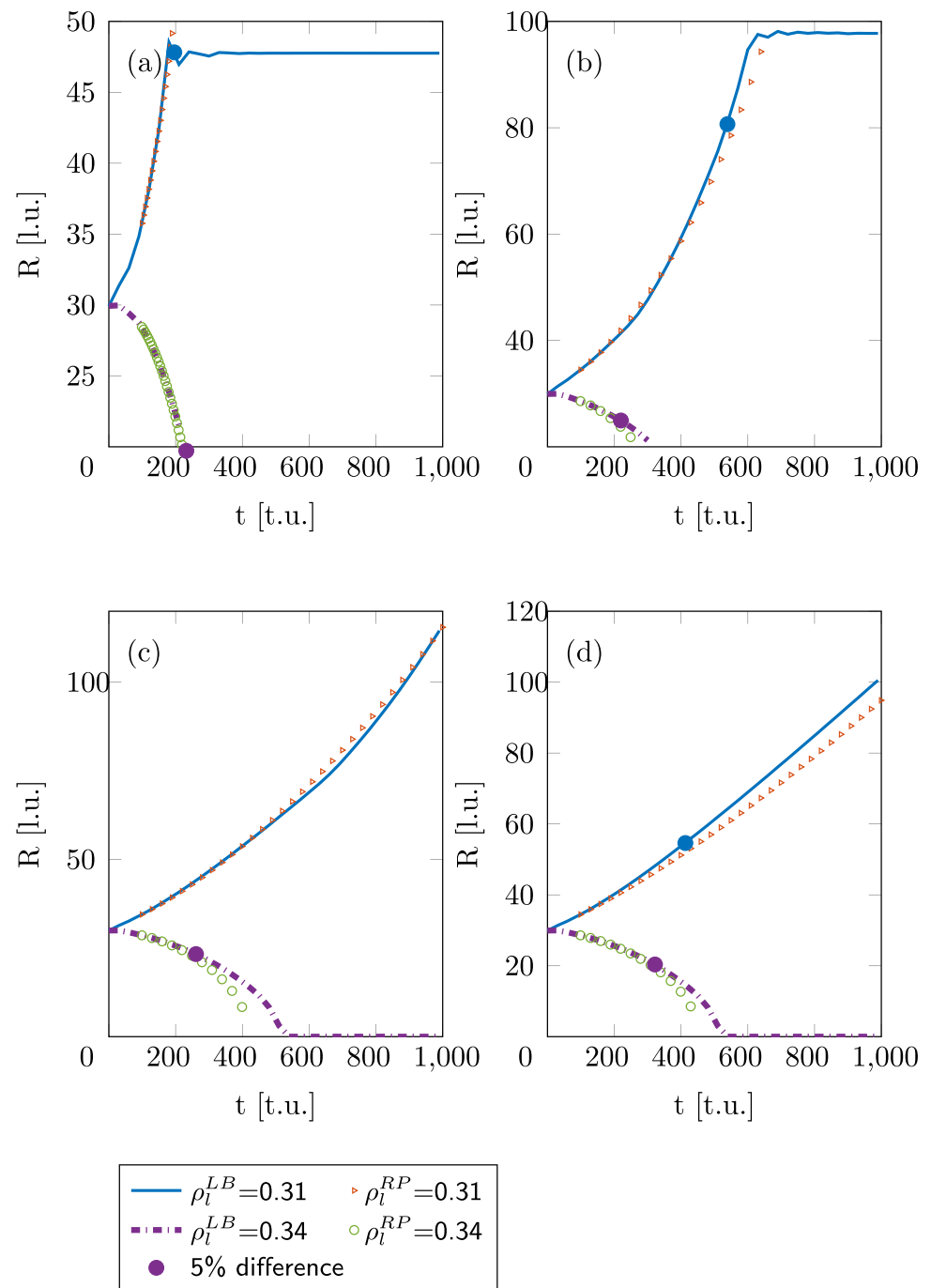
In the data delineated in Fig. 4, variations in domain size yield disparate results when compared with the R-P equation. Figure 4a–d present the outcomes associated with domain sizes of 100 [l.u.], 200 [l.u.], 400 [l.u.], and 1000 [l.u.], respectively. Specifically, we define a critical point for each domain size iteration: this is the juncture at which the relative difference of radius (ΔR) between the R-P equation's predictions and the LBM outcomes crosses a threshold of 5%. Notably, in the context of growth scenarios with the same R_∞ setting, the domain sizes of 400 [l.u.] and 100 [l.u.] exhibit inferior performance compared to those of 1000 [l.u.] and 200 [l.u.]. This outcome is unexpected and does not allow for the establishment of a clear relationship between the domain size and the overlap of the R-P and LBM simulations. Conversely, in collapse scenarios, a satisfactory match is observed only with the domain size of 100 [l.u.], suggesting that the radius is a primary influencing factor—a topic that warrants further investigation. For collapse cases, the influence of the boundary diminishes in larger domain sizes; hence, maintaining the same R_∞ setting leads to some discrepancies. Some previous publications reported similar discrepancies concerning the domain size [21] whereas others did not mention such issues [28]. In addition, a detailed rationale for this specific selection of domain dimensions was not provided. Furthermore, a comprehensive analysis of boundary effects was also not mentioned [1]. Nonetheless, this analysis underscores the necessity of careful consideration regarding the impact of boundaries, as their influence remains notable even in considerably large domains, particularly after a certain iteration threshold is surpassed.

The discrepancy observed in the final stages of collapse can be attributed to significant diffusion effects, particularly when the bubble diminishes to a minimal size. As illustrated in Fig. 5d, which shows a close-up contour, pronounced diffusion is evident during the collapse phase of the bubble. Furthermore, the choice of pressure averaging strategy contributes marginally to the variations in outcomes. For this study, a centred-pressure averaging strategy was employed to maintain simplicity in methods. In the modified R-P equation, the parameter R_∞ is adjusted due to the original formulation's assumption of an infinite boundary, which impacts the outcomes. It is conceivable that in existing literature [5, 23, 27, 28], this parameter has been fine-tuned to match the results of the R-P equation with those obtained from LBM simulations. However, no universally optimized parameter is applicable across all cases. The selection of the parameter in this article is based on an area-weighted length within a square domain.

3.5 The impact of radius

In the analysis of radius-related outcomes depicted in Fig. 6, a discernible trend is observed, whereby an increase in the radius correlates with a rise in the specific iterations required to achieve a 5% discrepancy of ΔR . This pattern is particularly pronounced when comparing a radius of 350 [l.u.] with one of 35 [l.u.], where the iterations necessary to reach the 5% difference threshold are significantly more extended for the larger radius. Notably, the relationship between the radius and the number of iterations appears to be almost linear. Furthermore, toward the end of the simulation, the radius difference consistently remains substantial, potentially attributable to the inadequate resolution when dealing with smaller bubbles. This observation underscores the pivotal role of radius in impacting the outcomes of simulations. This conclusion is in concordance with the findings presented by Ezzatneshan and Vaseghnia [22], who reported a decreasing discrepancy with increasing radius in the initial phases of their study. Similarly, the research by Peng et al. [1] on a growth case showed a marked deviation towards the end of the simulation, especially pronounced at smaller radii. In addition, at the end of the simulation, there is always a discrepancy, and this discrepancy increases with the number

Fig. 4 The impact of domain size on growth and collapse case for radius 30 [l.u.]. **a** domain size=100 [l.u.], **b** domain size=200 [l.u.], **c** domain size=400 [l.u.]. For this case of growth, the 5% threshold that was defined previously is not reached at the end of the simulation. **d** domain size=1000 [l.u.]



of iterations, regardless of the bubble's radius. The reason for this is partly because diffusion occurs at the end of the simulation, as shown in Fig. 5d.

Another reason for that is that this is a nonlinear phenomenon and initial differences are being amplified as time passes. The rapidly growing difference between the LBM and R-P predictions is clearly observable in Fig. 3c, d. It remains unclear to what extent this increasing difference is caused by the diffusing interface in the case of the LBM and other factors, such as the presence of weakly compressible effects in LBM. Furthermore, the study conducted by Gai et al. [27] also provides empirical evidence in support of this observation. Their findings, particularly in the context of the collapse case simulations, reveal discernible discrepancies between the results obtained from the LBM and those predicted by the R-P equation toward the end of the simulation. Additionally, the research conducted by

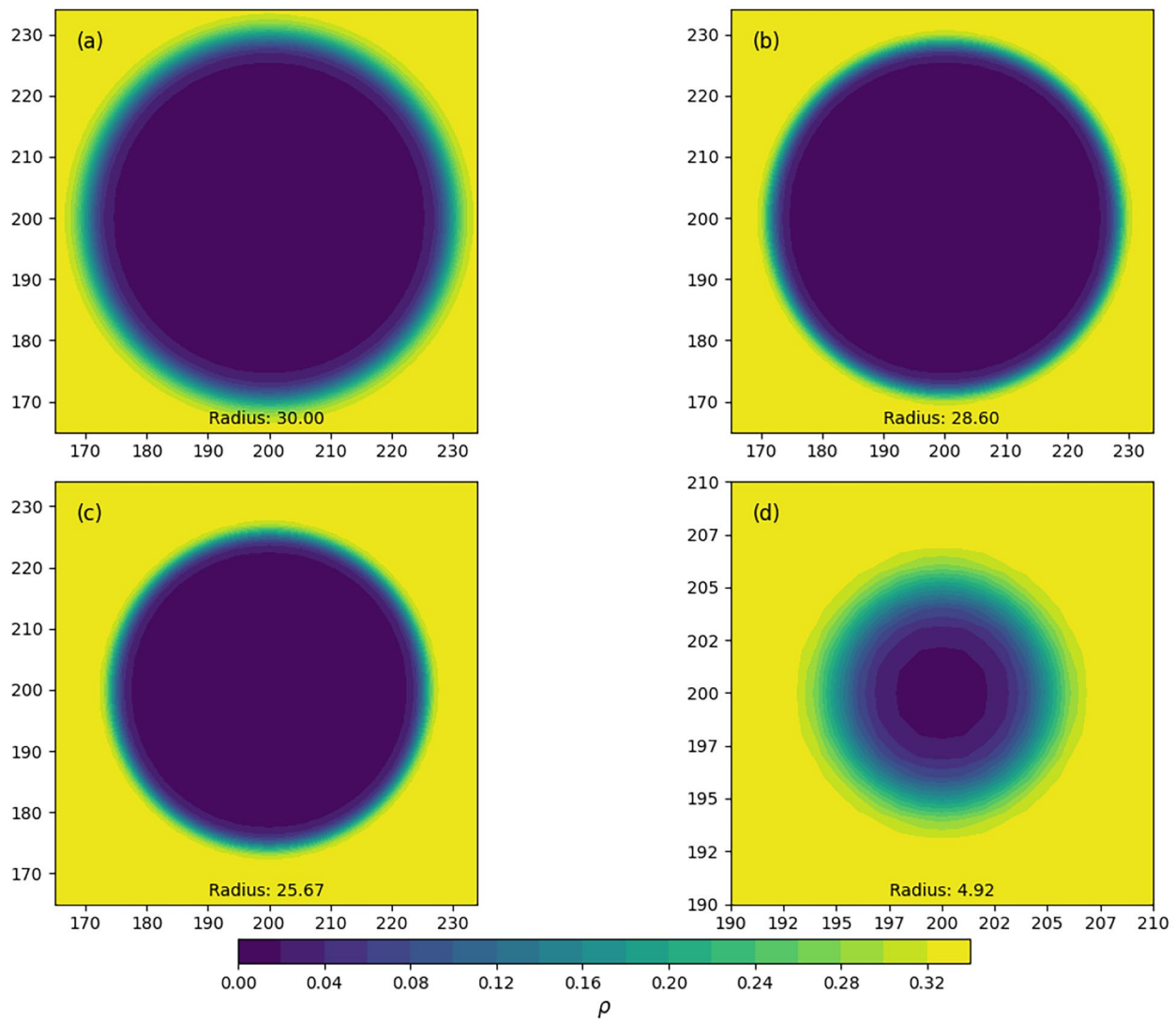


Fig. 5 density contour of the bubble with domain size 400 [l.u.] and initial radius=30 [l.u.]. **a** iteration=0 [t.u.], **b** iteration=100 [t.u.], **c** iteration=200 [t.u.], **d** iteration=500 [t.u.]

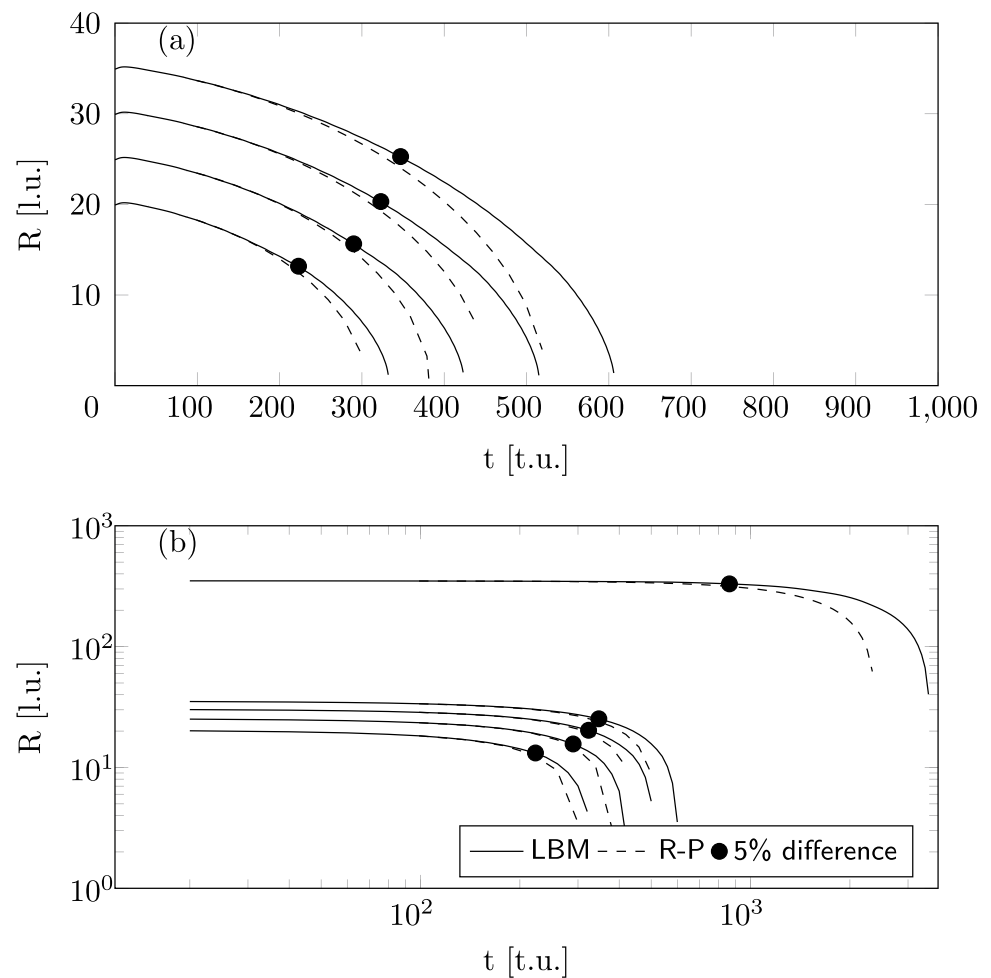
Peng et al. [23] provides further evidence of this phenomenon. Particularly in the collapse case simulations, their findings exhibit certain discrepancies.

4 Conclusions

This article performed the LBM simulation of a single bubble based on the Shan-Chen Model. Then validate the results against Laplace's law, Maxwell's area construction, and R-P equation. Based on the provided results and discussion, the following conclusion can be drawn,

- Good agreements were found in Laplace's law and Maxwell's area construction benchmark cases but not in the R-P equation case.
- Integrating initial conditions from the LBM into the R-P equation at time zero ($t=0$ t.u.) shows a notable discrepancy between the models, highlighting the R-P equation's sensitivity to initial states from LBM simulations. However,

Fig. 6 The impact of radius with domain size $L_x = L_y = 1000$ [l.u.] and initial condition from LBM at time 100 [t.u.] **a** radius from 20 to 35 [l.u.], **b** log-log plot of radius including 20, 25, 30, 35, 350 [l.u.]



using initial conditions from LBM at time 100 [t.u.] significantly improves model alignment, whereas starting from time 150 [t.u.] offers minimal additional benefit. This indicates that while using later initial conditions from LBM reduces discrepancies with the R-P equation, the improvement plateaus, making the initial condition at time 100 [t.u.] optimal for balancing model agreement and efficiency.

- The domain size and the parameter R_∞ play pivotal roles in aligning the results between the LBM and the R-P equation. The parameter R_∞ defines the distance from the center of the bubble to the domain boundary. Notably, in LBM, the domain is square, whereas it is cylindrical in the context of the R-P equation. This discrepancy leads to a difference in the influence of the boundary of the domain between LBM and the R-P equation. However, there are no established methods for determining the optimal value of R_∞ . It has been observed that there is no universally optimal R_∞ that is applicable across all domain sizes, as each domain size uniquely influences the outcomes. The literature suggests that authors may fine-tune R_∞ to achieve congruence between the LBM and R-P equation results.
- An analysis of the simulation data reveals an approximately linear relationship between the radius and the iteration at which the difference between the LBM and the R-P equation reaches a 5% threshold. Furthermore, a consistent observation towards the end of the simulation is the presence of a significant discrepancy. This is partly attributed to the insufficient resolution within the bubble when it becomes exceedingly small. However, bubble diffusion at small radii does not explain the discrepancies which are growing rapidly as a function of time even in the case of large bubbles

This study serves as a foundational exploration preceding future endeavours in simulating bubble cluster dynamics.

Acknowledgements We would like to acknowledge the IT support for using the High-Performance Computing (HPC) facilities at Cranfield University, UK. We would also like to acknowledge the assistance provided by ChatGPT, an AI developed by OpenAI, which was instrumental in proofreading the manuscript and suggesting improvements in language and structure.

Funding This research received no external funding.

Data availability The software required to reproduce the results is publicly available from <http://doi.org/10.5281/zenodo.10954690>.

Declarations

Competing interests The authors declare no competing interests.

Open Access This article is licensed under a Creative Commons Attribution 4.0 International License, which permits use, sharing, adaptation, distribution and reproduction in any medium or format, as long as you give appropriate credit to the original author(s) and the source, provide a link to the Creative Commons licence, and indicate if changes were made. The images or other third party material in this article are included in the article's Creative Commons licence, unless indicated otherwise in a credit line to the material. If material is not included in the article's Creative Commons licence and your intended use is not permitted by statutory regulation or exceeds the permitted use, you will need to obtain permission directly from the copyright holder. To view a copy of this licence, visit <http://creativecommons.org/licenses/by/4.0/>.

References

1. Peng C, Tian S, Li G, Sukop MC. Simulation of multiple cavitation bubbles interaction with single-component multiphase Lattice Boltzmann method. *Int J Heat Mass Transfer*. 2019;137:301–17.
2. Ogloblina D, Schmidt J, Adams NA. Simulation and analysis of collapsing vapor-bubble clusters with special emphasis on potentially erosive impact loads at walls, in: EPJ Web of Conferences, Vol. 180, EDP Sciences, 2018, p. 02079.
3. Shang X, Huang X. Investigation of the dynamics of cavitation bubbles in a microfluidic channel with actuations. *Micromachines*. 2022;13(2):203.
4. Koch M, Lechner C, Reuter F, Köhler K, Mettin R, Lauterborn W. Numerical modeling of laser generated cavitation bubbles with the finite volume and volume of fluid method, using OpenFOAM. *Comput Fluids*. 2016;126:71–90.
5. Peng C, Tian S, Li G, Sukop MC. Simulation of laser-produced single cavitation bubbles with hybrid thermal lattice Boltzmann method. *Int J Heat Mass Transfer*. 2020;149: 119136.
6. Chang C, Yang C, Lin F, Chiu T, Lin C. Lattice Boltzmann simulations of bubble interactions on GPU cluster. *J Chin Instit Eng*. 2021;44(5):491–500.
7. Shan M, Yang Y, Zhao X, Han Q, Yao C. Investigation of cavitation bubble collapse in hydrophobic concave using the pseudopotential multi-relaxation-time Lattice Boltzmann Method. *Chin Phys B*. 2021;30(4): 044701.
8. Ba Y, Liu H, Li Q, Kang Q, Sun J. Multiple-relaxation-time color-gradient Lattice Boltzmann model for simulating two-phase flows with high density ratio. *Phys Rev E*. 2016;94(2): 023310.
9. Leclaire S, Pellerin N, Reggio M, Trépanier J-Y. Enhanced equilibrium distribution functions for simulating immiscible multiphase flows with variable density ratios in a class of Lattice Boltzmann models. *Int J Multiphase Flow*. 2013;57:159–68.
10. Huang H, Huang J-J, Lu X-Y, Sukop MC. On simulations of high-density ratio flows using color-gradient multiphase Lattice Boltzmann models. *Int J Modern Phys C*. 2013;24(04):1350021.
11. Reis T, Phillips TN. Lattice Boltzmann model for simulating immiscible two-phase flows. *J Phys A Math Theor*. 2007;40(14):4033.
12. Banari A, Janßen C, Grilli ST, Krafczyk M. Efficient GPGPU implementation of a Lattice Boltzmann model for multiphase flows with high density ratios. *Comput Fluids*. 2014;93:1–17.
13. Verdier W, Kestener P, Cartalade A. Performance portability of Lattice Boltzmann methods for two-phase flows with phase change. *Comput Methods Appl Mech Eng*. 2020;370: 113266.
14. Yang L, Shu C, Chen Z, Wang Y, Hou G. A simplified Lattice Boltzmann flux solver for multiphase flows with large density ratio. *Int J Num Methods Fluids*. 2021;93(6):1895–912.
15. Liang H, Shi B, Guo Z, Chai Z. Phase-field-based multiple-relaxation-time lattice Boltzmann model for incompressible multiphase flows. *Physical Review E*. 2014;89(5): 053320.
16. Liang H, Xu J, Chen J, Wang H, Chai Z, Shi B. Phase-field-based lattice Boltzmann modeling of large-density-ratio two-phase flows. *Phys Rev E*. 2018;97(3): 033309.
17. Yuan J, Weng Z, Shan Y. Modelling of double bubbles coalescence behavior on different wettability walls using LBM method. *Int J Therm Sci*. 2021;168: 107037.
18. Liu Y, Peng Y. Study on the collapse process of cavitation bubbles including heat transfer by lattice Boltzmann Method. *J Marine Sci Eng*. 2021;9(2):219.
19. Yuan X, He X, Wang K. Numerical simulation of effects of vapor and liquid phase viscosity coefficients on cavitation bubble collapse process. *Adv Sci Technol Water Res*. 2020;40(5):19–23.
20. Mao Y, Peng Y, Zhang J. Study of cavitation bubble collapse near a wall by the modified Lattice Boltzmann method. *Water*. 2018;10(10):1439.
21. Shi Y-Z, Luo K, Chen X-P, Li D-J. A numerical study of the early-stage dynamics of a bubble cluster. *J Hydrodyn*. 2020;32:845–52.
22. Ezzatneshan E, Vaseghnia H. Dynamics of an acoustically driven cavitation bubble cluster in the vicinity of a solid surface, *Physics of Fluids*. 2021; 33 (12).

23. Peng C, Tian S, Li G, Sukop MC. Single-component multiphase Lattice Boltzmann simulation of free bubble and crevice heterogeneous cavitation nucleation. *Phys Rev E*. 2018;98(2): 023305.
24. Krüger T, Kusumaatmaja H, Kuzmin A, Shardt O, Silva G, Viggien EM. *The Lattice Boltzmann method*. Berlin: Springer International Publishing; 2017. p. 4–15.
25. Mohamad A. *Lattice Boltzmann method*. Berlin: Springer; 2011.
26. Shan X, Chen H. Lattice Boltzmann model for simulating flows with multiple phases and components. *Phys Rev E*. 1993;47(3):1815.
27. Gai S, Peng Z, Moghtaderi B, Yu J, Doroodchi E. LBM study of ice nucleation induced by the collapse of cavitation bubbles. *Comput Fluids*. 2022;246: 105616.
28. Ezzatneshan E, Vaseghnia H. Simulation of collapsing cavitation bubbles in various liquids by Lattice Boltzmann model coupled with the Redlich-Kwong-Soave equation of state. *Phys Rev E*. 2020;102(5): 053309.
29. Kuzmin A, Mohamad A. Multirange multi-relaxation time Shan-Chen model with extended equilibrium. *Comput Math Appl*. 2010;59(7):2260–70.
30. Brennen CE. *Cavitation and bubble dynamics*. Cambridge: Cambridge University Press; 2014.
31. MATLAB R2022a, Natick, Massachusetts, United States (2022). <https://www.mathworks.com>
32. Dormand JR, Prince PJ. A family of embedded Runge-Kutta formulae. *J Comput Appl Math*. 1980;6(1):19–26.
33. Chapman S, Cowling TG. *The mathematical theory of non-uniform gases: an account of the kinetic theory of viscosity, thermal conduction and diffusion in gases*. Cambridge: Cambridge University Press; 1990.
34. Baakeem SS, Bawazeer SA, Mohamad AA. A novel approach of unit conversion in the lattice Boltzmann method. *Appl Sci*. 2021;11(14):6386.
35. Porter ML, Coon E, Kang Q, Moulton J, Carey J. Multicomponent interparticle-potential Lattice Boltzmann model for fluids with large viscosity ratios. *Phys Rev E*. 2012;86(3): 036701.
36. Liu M, Yu Z, Wang T, Wang J, Fan L-S. A modified pseudopotential for a Lattice Boltzmann simulation of bubbly flow. *Chem Eng Sci*. 2010;65(20):5615–23.
37. Huang J, Yin X, Killough J. Thermodynamic consistency of a pseudopotential Lattice Boltzmann fluid with interface curvature. *Phys Rev E*. 2019;100(5): 053304.

Publisher's Note Springer Nature remains neutral with regard to jurisdictional claims in published maps and institutional affiliations.

2024-05-01

Critical assessment of the lattice Boltzmann method for cavitation modelling based on single bubble dynamics

Xiong, Xin

Springer

Xiong X, Teschner TR, Moulitsas I, et al. (2024) Critical assessment of the lattice Boltzmann method for cavitation modelling based on single bubble dynamics. *Discover Applied Sciences*, Volume 6, Issue 5, May 2024, Article number 241

<https://doi.org/10.1007/s42452-024-05895-1>

Downloaded from Cranfield Library Services E-Repository